DEUTSCHES ELEKTRONEN-SYNCHROTRON **DESY**

DESY 83-017
LAL 83-2
March 1983

受入
83-5-79
高エ研図書室

LEPTON PAIR PRODUCTION IN DEEP INELASTIC e-γ SCATTERING

by

CELLO Collaboration

ISSN 0418-9833

NOTKESTRASSE 85 · 2 HAMBURG 52

DESY behält sich alle Rechte für den Fall der Schutzrechtserteilung und für die wirtschaftliche Verwertung der in diesem Bericht enthaltenen Informationen vor.

DESY reserves all rights for commercial use of information included in this report, especially in case of filing application for or grant of patents.

To be sure that your preprints are promptly included in the
HIGH ENERGY PHYSICS INDEX ,
send them to the following address (if possible by air mail) :

DESY
Bibliothek
Notkestrasse 85
2 Hamburg 52
Germany

DESY 83-017
LAL 83-2
March 1983

ISSN 0418-9833

LEPTON PAIR PRODUCTION IN DEEP INELASTIC e–γ SCATTERING

by

the CELLO Collaboration

ABSTRACT

At PETRA we have measured the process $e + \gamma \rightarrow e + \ell^+ + \ell^-$, where ℓ is either an electron or a muon, at an average Q^2 of 9.5 GeV^2/c^2. The total number of collected events is 240. We find that our data agree with QED predictions based either on exact Feynman graph calculations or on the photon structure function expressions.

CELLO Collaboration

H.-J. Behrend, H. Fenner, U. Gümpel, M.-J. Schachter[1],
V.Schröder, H. Sindt
Deutsches Elektronen-Synchrotron, DESY, Hamburg, Germany

G. D'Agostini, W.-D. Apel, S. Banerjee[2], J. Bodenkamp, J. Engler,
G. Flügge, D.C. Fries, W. Fues, K. Gamerdinger, G. Hopp, H. Küster
H. Müller, H. Randoll, G. Schmidt, H. Schneider
Kernforschungszentrum Karlsruhe and Universität Karlsruhe, Germany

W. de Boer, G. Buschhorn, G. Grindhammer, P. Grosse-Wiesmann,
B. Gunderson, C. Kiesling, R. Kotthaus, U. Kruse[3], H. Lierl,
D. Lüers, H. Oberlack, P. Schacht
Max-Planck-Institut für Physik und Astrophysik, München, Germany

G. Carnesecchi[4], P. Colas, A. Cordier, M. Davier, D. Fournier,
J.-F. Grivaz, J. Haïssinski, V. Journé, F. Laplanche,
F. Le Diberder, U. Mallik, J.-J. Veillet
Laboratoire de l'Accélérateur Linéaire, Orsay, France

J.H. Field[5], R. George, M. Goldberg, B. Grossetête, O. Hamon,
F. Kapusta, F. Kovacs, G. London, L. Poggioli, M. Rivoal
Laboratoire de Physique Nucléaire et des Hautes Energies,
Université de Paris, France

R. Aleksan, J. Bouchez, G. Cozzika, Y. Ducros, A. Gaidot,
Y. Lavagne, J. Pamela, J.-P. Pansart, F. Pierre
Centre d'Etude: Nucléaires, Saclay, France

---

1) Present address : Waitzstrasse 43, Hamburg 52.

2) Now at Tata Institute, Bombay, India.

3) Visitor from the University of Illinois, Urbana, USA.

4) Now at Centre d'Etudes Nucléaires, Saclay, France.

5) On leave of absence from DESY, Hamburg, Germany.

I. Introduction

Using data collected at the e^+e^- storage ring PETRA at DESY in 1980 and 1981, the CELLO Collaboration has investigated deep inelastic e-γ scattering (DIS) along three lines :

(I) lepton pair production at medium Q^2 values ($\langle Q^2 \rangle \sim 10$ GeV^2/c^2) where Q^2 is the four momentum transfer squared of the scattered electron,

(II) measurement of the hadronic photon structure function $F_2(x,Q^2)$ in the same Q^2 range,

(III) study of hadronic DIS events at very high Q^2 ($\langle Q^2 \rangle \sim 100$ GeV^2/c^2).

This letter presents the first part of this program while the second part is described in the next letter[1]. Results on the high Q^2 hadronic events have been published previously[2].

We report here on the purely leptonic reactions

$$e + \gamma \rightarrow e + e^+ + e^- , \tag{1}$$

$$e + \gamma \rightarrow e + \mu^+ + \mu^- \tag{2}$$

where the three final leptons are detected. The process which actually takes place in the storage ring is

$$e^+ + e^- \rightarrow e^+ + e^- + \ell^+ + \ell^- , \ (\ell = e, \mu). \tag{3}$$

Only very limited experimental results have been reported[3,4] up to now on this process when one of the scattered electrons is detected at large angles. To a very good approximation, the cross section, of order α^4, is given[5] by the two Feynman graphs shown in Fig. 1a. The Vermaseren integration program[6] allows to take

into account 4 other graphs (see Fig. 1b) which describe virtual bremsstrahlung in the t-channel of Bhabha scattering. The contribution of virtual bremsstrahlung in the s-channel is negligible.

II. The CELLO detector

A detailed description of CELLO can be found in Ref.7. The scattered electron of reaction (1) or (2) is tagged by an end cap electromagnetic calorimeter. The latter consists of 4 liquid argon modules which accept polar angles ranging between .130 and .400 rad and provide an almost complete azimuthal coverage. The resolution of these modules has been determined by analyzing Bhabha scattering events collected at E_{beam} = 17 GeV. For such events we have found a 6% energy resolution and a 4 mrad angular resolution when the shower develops away from the module edges. Monte-Carlo calculations show that the energy resolution drops to about 15 % when the electron energy is only 7 GeV and edge effects are taken into account. The latter resolution value has been checked by a detailed study of radiative Bhabha events where the photon is detected in an end cap module.

Both particles of the lepton pair (e^+e^- or $\mu^+\mu^-$) in reaction (1) or (2) are detected in a set of 12 cylindrical wire chambers placed in a 1.3 T magnetic field. The momentum resolution of this tracking device, which includes 7 drift chambers, is σ_{p_T}/p_T = 2% P_T (P_T in GeV/c) where p_T is the transverse momentum with respect to the beam. We demand at least 7 hits per track. This requirement implies the cut $|\cos(\Theta)| < .92$.

These chambers are surrounded by a barrel liquid argon calorimeter which is 20 radiation lengths thick. Its angular acceptance is $|\cos\Theta| < .86$. Read out strips in 3 different directions (longitudinal, transverse and 45°) allow for shower reconstruction with an angular precision of 4 mrad and an energy resolution σ_E/E = 13 %/$\sqrt{E}$ (GeV).

Muons are detected in drift chambers located behind 5 to 6 absorption lengths of iron. They cover 92 % of 4π.

The trigger used for these measurements is activated by two charged particles with p_T > .250 GeV/c in the central chambers *or* by an end cap shower above 3 GeV combined with either a charged particle in the central chambers or an energy deposition of more than 3 GeV in the barrel calorimeter.

III. Data collection and event selection

The data used in this analysis were collected at an average beam energy of 17 GeV for an integrated luminosity of 7.5 pb^{-1}.

The event selection starts with a search for *single* isolated showers in the end cap modules. These showers are required to have an energy above 3.6 GeV and a polar angle .140 < θ < .370 rad. It follows that Q^2_{min} = 1.2 GeV^2/c^2. A Monte-Carlo simulation shows that, within such cuts, the tagging efficiency is 92%, taking into account losses in the shower reconstruction stage.

We then demand two and only two tracks of opposite charge in the central detector originating from the interaction region defined by |z| < 3.5 cm and r < 2 cm. These tracks must satisfy P_T > .120 GeV/c. This cut is introduced by the tracking program. Events which include an electromagnetic shower in addition to the two charged particles in the central detector are kept when such a shower can be linked to one of the tracks.

Next, we check the visible transverse momentum balance in order to reject DIS events with $\tau^+\tau^-$ or multihadron production. We first apply a loose cut at 2.8 GeV/c to the sum $|\vec{P}_{Te} + \vec{P}_{T1} + \vec{P}_{T2}|$ of the transverse momenta of the tagged electron and of the two particles measured in the central detector. We further demand that $\vec{P}_{Te}$ be back to back within ± .6 rad with the combined transverse momentum $\vec{P}_{T1} + \vec{P}_{T2}$ of the large angle tracks.

Finally, only those events which satisfy $W^2 > 1$ GeV$^2/c^4$ are kept where W is the invariant mass of the $\ell^+\ell^-$ system.

IV - Particle identification

In a preliminary analysis, a sample of 111 muon events has been obtained by using the muon chambers. The main characteristics of these events have been briefly reported in Ref. 8. This sample has been used to cross-check a second identification procedure which is based on a detailed analysis of the energy deposition in the barrel liquid argon calorimeter and which allows the selection of electrons and muons separately. In this analysis, the fiducial volume is restricted well within the liquid argon stacks, and $\ell^\pm$ tracks with a momentum greater than .8 GeV/c are the only ones used. 399 events have at least one track which meets these requirements. 158 of them are easily recognized as being either $e^+e^- \rightarrow e^+e^- \gamma$ radiative Bhabha scattering events or $e^+e^- \rightarrow \mu^+\mu^-\gamma$ radiative annihilation events where the photon simulates a tagged electron in the end cap modules. Indeed, these events have a good *total* momentum balance and a total visible energy (end cap shower + 2 central track energies) greater than 75% of $2E_{beam}$ Their number and their kinematical characteristics agree well with the predictions of the Berends and Kleiss[9] program. For the rejection of such events we do not rely on a single cut but we require that at least two criteria be met among a set of 4 which involves the event total energy, the total momentum, the degree of coplanarity of the 3 tracks and the higher of the 2 central track momenta.

The identification of the particle as an electron or a muon is then based on the longitudinal distribution of the total charge q collected in the liquid argon stacks and on the ratio q/P, where P is the particle momentum as measured with the central chambers. The analysis of events where both central particles can be submitted to this identification procedure (about 1/3 of the total sample), together with a study of a sample of cosmic rays and a sample of e^+e^- pairs produced by γ conversions in the beam pipe shows that misidentifications occur at a level which is below 3%.

It will be seen below that the pion contamination is expected to represent less than 1 % of the total sample of events. Therefore no attempt has been made to recognize pion tracks, i.e. they have been categorized either as electron tracks or as muon tracks. Subtractions based on Monte Carlo simulations have been made to correct for this contamination.

This selection leads to 130 electronic DIS candidates and 111 muonic candidates*. All candidates and a fraction of those events which are rejected by the selection procedure have been scanned.

V - Background

The background to the $e^+e^- \to e^+e^- \ell^+\ell^-$ process may originate in (i) e γ DIS leading to $\tau^+ \tau^-$ production, (ii) e γ DIS leading to multihadron production where only two particles are seen in the central detector, or (iii) radiative annihilation events $e^+e^- \to X \gamma$ where X is either a lepton pair or a multihadron final state and where the photon or a π^0 (in the X = multihadron case) fakes a tagged electron.

As far as the $e^+e^- \to e^+e^-\pi^+\pi^-$ two-photon reaction is concerned, single tag studies[10,11] of f° production at $Q^2 \sim 0.3$ GeV^2/c^2 and an upper limit[12] put on the $\pi^+\pi^-$ continuum investigated at $.1 < Q^2 < 10.0$ GeV^2/c^2 and $W > 2.0$ GeV/c^2 indicate that this process is rapidly suppressed when one of the photons becomes virtual. By extrapolating these results to our kinematical region, we find that we may neglect this exclusive $\pi^+\pi^-$ production with respect to the $\ell^+\ell^-$ yield.

---

* It so happens that this muon sample has precisely the same size as the one previously obtained with the muon chambers. The intersection of these two samples represents 75 % of either of them. This fraction agrees with what is expected from the differences in phase space acceptance of the two selection methods.

Each one of the above background sources has been simulated by Monte-Carlo programs. The Berends and Kleiss[9] program has been used for the radiative processes. Within our tagging acceptance, the total cross section of process (i) is one order of magnitude lower than that of reaction (1) or reaction (2). The P_T cuts further reduce the background due to this process to a negligible amount. As far as process (ii) is concerned, its total cross section is comparable to those of reactions (1) or (2) but the low multiplicity requirement combined with the P_T cuts are quite effective in eliminating such events and the subtraction implied by this contamination is just one event. It also turns out that, within our cuts, the background due to process (iii) is negligible.

The virtual bremsstrahlung contribution to the cross section has been calculated with the Vermaseren program. Because of the $W^2 > 1\ GeV^2/c^4$ cut, this contribution is less than 1%. Nevertheless, we have also examined the possibility of a forward backward asymmetry originating from the interference between the graphs of Fig. 1a and those of Fig. 1b which differ by the C value of the $\ell^+\ell^-$ pair. We define NF (resp. NB) the number of leptons ℓ which are detected in the forward (resp. backward) hemisphere with respect to the direction of the beam which carries the same electric charge as ℓ. It turns out that numerical integration by the Vermaseren routine leads to a value of A = (NF - NB) / (NF + NB) less than 2% for both electrons* and muons under our experimental conditions. The data show some positive asymmetry in both lepton final states but are compatible, within statistics, with the results of the Vermaseren program. We consider that this point should be further investigated when more data will be available.

---

* The complete antisymmetrization of the 4 $e^{\pm}$ final state is not performed in the $e^+ + e^- \to e^+ + e^- + e^+ + e^-$ case.

VI - Comparison of the data with QED predictions

Once the backgrounds are subtracted, our data are compared to theoretical expectations drawn either from the Vermaseren program or from a Monte-Carlo program which makes use of the photon structure functions $F_{1,2}(x,W^2)$. In fact we find negligible differences between these two approaches when three precautions are taken in the calculations based on the structure functions :

(i) The angle dependent expression[13,14] is used for the target photon flux. We obtain such an expression by differentiating the following formula with respect to the electron scattering angle θ_e

$$\frac{dn}{dx_1} = \frac{\alpha}{\pi} \frac{1}{x_1} \left\{ \left[1 + (1-x_1)^2 \right] \ln \left[2 \frac{E_{beam}}{m_e} \frac{(1-x_1)}{x_1} \sin\left(\frac{\theta_e}{2}\right) \right] - 1 + x_1 \right\}$$

where $x_1 = E_\gamma / E_{beam}$. This formula gives the photon flux integrated over the electron scattering angle up to θ_e.

(ii) Off-mass-shell effects are included. We use the following expression[5] for the F_2 structure function

$$F_2 = \frac{\alpha}{\pi} x \left(\left(x^2 + (1-x)^2 \right) \ln \left(\frac{W^2}{m_\ell^2 + tx(1-x)} \right) - 1 + 8x(1-x) - \frac{tx(1-x)}{m_\ell^2 + tx(1-x)} \right)$$

$x = \frac{Q^2}{Q^2+W^2}$ is the standard scaling variable and $t = -k^2$ where k is the target photon 4-momentum (the presence of the t dependent corrections reduces the total cross section by as much as 45% in the case of reaction (1) and by 12% in the case of reaction (2) under our experimental conditions).

(iii) The $\gamma + \gamma \to \ell^+ \ell^-$ angular distribution --which has to be introduced since the detector acceptance does not cover the full $\ell^+\ell^-$ production-- takes into account the fact that the two photons are virtual : in these conditions the angular distribution of the final leptons is less peaked than it would be in the case of two real photons sharing the same total center of mass energy.

We have investigated the consequences of real photon emission by the incoming electron (see left hand side of reaction (1) or (2)). We have found that this emission implies a 4% radiative correction which has been applied to the theoretical predictions.

Since the electron and muon kinematical distributions are very much alike in our acceptance region we do not present separate plots. Fig. 2 compares the uncorrected data to predictions based on theory and a detailed detector simulation for the lepton momenta and for the acollinearity angle. Notice that in Fig. 2a *both* the electron and the muon momentum distributions have two peaks at about the same values. Data and theory are also compared in Fig.3 where the W^2 and the Q^2 distributions are displayed. The average Q^2 is 9.5 GeV^2/c^2.

As far as absolute yields are concerned, we expect from QED and the detector simulation 122 ± 9.5 and 110.5 ± 8.5 events for reactions (1) and (2) respectively while we observe 130 ± 11.4 and 110 ± 10.5. The error attached to the theoretical numbers takes into account uncertainties concerning the luminosity, the detection efficiency and radiative corrections which have only been partially applied.

VII - Results concerning F_2

When applied to reactions (1) or (2) the structure function formalism gives an insight into the lepton content of the photon. This formalism deals with the cross section integrated over the whole $\ell^+\ell^-$ phase space, while in practice a fraction of the DIS events is very difficult to observe, since one of the two leptons tends to be lost in the beam pipe. In such an analysis, the fact that electrons are much lighter than muons has three consequences: (i) the total e^+e^- yield which corresponds to our tagging acceptance is about twice the $\mu^+\mu^-$ yield ; (ii) the fraction of leptons which are lost in the beam pipe is larger in the e^+e^- case ; we observe 13 % of all events for reaction (1) and 22 % for

reaction (2); (iii) the corrections to F_2 due to the non vanishing mass of the target photon are much larger for the electrons (numbers are given above). It follows from (ii) and (iii) that we do not give results concerning F_2 in the e^+e^- case. In the $\mu^+\mu^-$ case, the extrapolation needed to determine F_2 appears safe as long as the angular distribution modification mentioned above -which is small for reaction (2)- is taken into account. Thus, from the dn/dx distribution of the muonic events, we infer results concerning F_2 as shown in Fig. 4. The curve and the experimental points shown in this figure represent F_2 (x, Q^2) values averaged over the observed Q^2 distribution. The theoretical curve is an absolute prediction. There is an overall 8% uncertainty on the experimental points mainly due to luminosity, acceptance and detection efficiency errors.

VIII - Conclusion

We have observed a high order QED process ($\sigma \propto \alpha^4$) at an average Q^2 of 9.5 GeV^2/c^2. Our data agree with exact Feynman graph calculations. Good agreement is also obtained with the structure function formalism which indicates that we have a good basis to investigate the hadronic photon structure function[1].

ACKNOWLEDGMENTS.

We would like to thank M. Defrise and P. Kessler for fruitfull discussions. We are indebted to the PETRA machine group for its excellent support during the experiments. We acknowledge the invaluable effort of all engineers and technicians of the collaborating institutions in the construction and maintenance of the apparatus, in particular the operation of the magnet system by G. Mayaux and Dr. Horlitz and their groups. The visiting groups wish to thank the DESY directorate for the support and kind hospitality extended to them.

REFERENCES

1) CELLO Collaboration, H.-J. Behrend et al., Phys. Lett. (see next letter).

2) CELLO Collaboration, H.-J. Behrend et al., Phys. Lett. 118B (1982) 211.

3) PLUTO Collaboration, Proceedings of the XXth International Conference on High Energy Physics, Madison (1980), published by the American Institute of Physics.

4) MARK-J Collaboration, B. Adeva et al., Phys. Rev. Lett. 48 (1982) 721.

5) V.M. Budnev et al., Phys. Reports 15C (1975) 181.

6) R. Bhattacharya, J. Smith and G. Grammer, Jr, Phys. Rev. D15 (1977) 3267.
J.A.M. Vermaseren, Proceedings of the International Workshop on $\gamma\gamma$ collisions, Amiens (1980), published by Springer-Verlag.

7) CELLO Collaboration, H.-J. Behrend et al., Phys. Scripta 23 (1981) 610.

8) J. Haïssinski (CELLO), XVIIth Rencontre de Moriond, vol. II (1982), published by Editions Frontières.
CELLO Collaboration, H.-J. Behrend et al., Proceedings of the XXIst International Conference on High Energy Physics, Paris (1982), published by Les Editions de Physique.

9) F.A. Berends and R. Kleiss, Nucl. Phys. B177 (1981) 237.

10) PLUTO Collaboration, Ch. Berger et al., Phys. Lett. 94B (1980) 254.

11) TASSO Collaboration, R. Brandelik et al., DESY Report 81/026 (1981).

12) PLUTO Collaboration, Ch. Berger et al., Nucl. Phys. B202 (1982) 189.

13) N. Arteaga-Romero, A. Jaccarini and P. Kessler, Phys. Rev. D3 (1971) 1569.

14) J.H. Field, Nucl. Phys. B168 (1980) 477 (E: B176 (1980) 545).
Ch. Berger and J.H. Field, Nucl. Phys. B187 (1981) 585.

FIGURE CAPTIONS

Fig. 1 a) Feynman graphs of the deep inelastic e–γ scattering process.

b) Feynman graphs of virtual bremsstrahlung in the t-channel of Bhabha scattering.

Fig. 2 a) Lepton momentum distribution in deep inelastic e–γ scattering. Comparison between data and QED prediction.

b) Lepton acollinearity angle distribution compared with QED prediction

Fig. 3 a) W^2 distribution of lepton pairs produced in deep inelastic e–γ scattering. Comparison between data and QED prediction.

b) Q^2 distribution compared with QED prediction.

Fig. 4 Comparison between the theoretical and the measured values of F_2 (x) for the reaction $e+\gamma \rightarrow e + \mu^+ + \mu^-$. The values of F_2 have been averaged over the Q^2 distribution which corresponds to the CELLO tagging acceptance (cf. Fig. 3b). In this figure, the theoretical curve and the experimental points are absolute ones (they have not been normalized to each other).

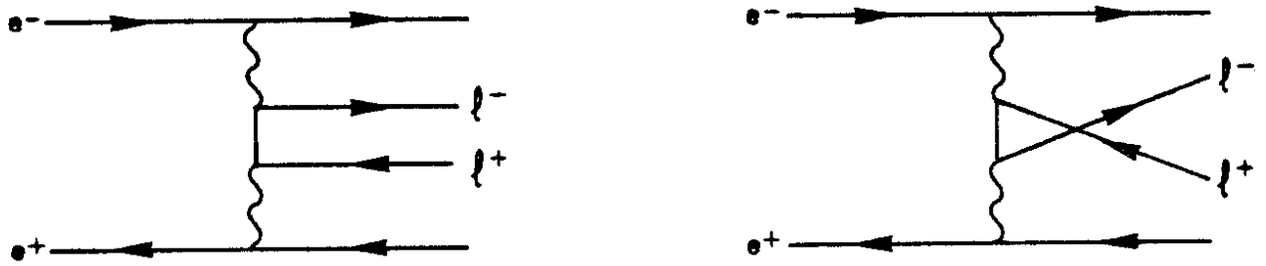

Fig. 1a

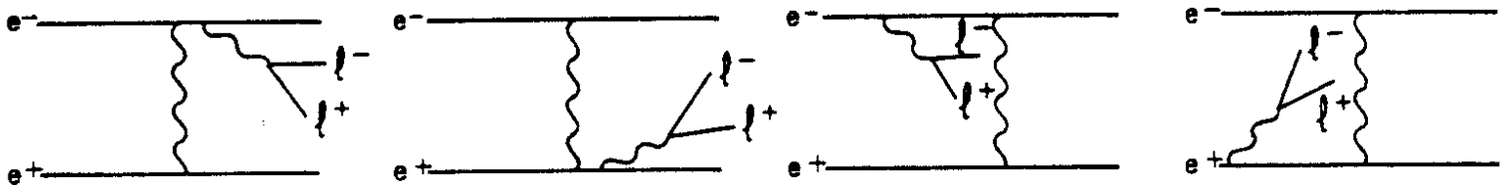

Fig. 1b

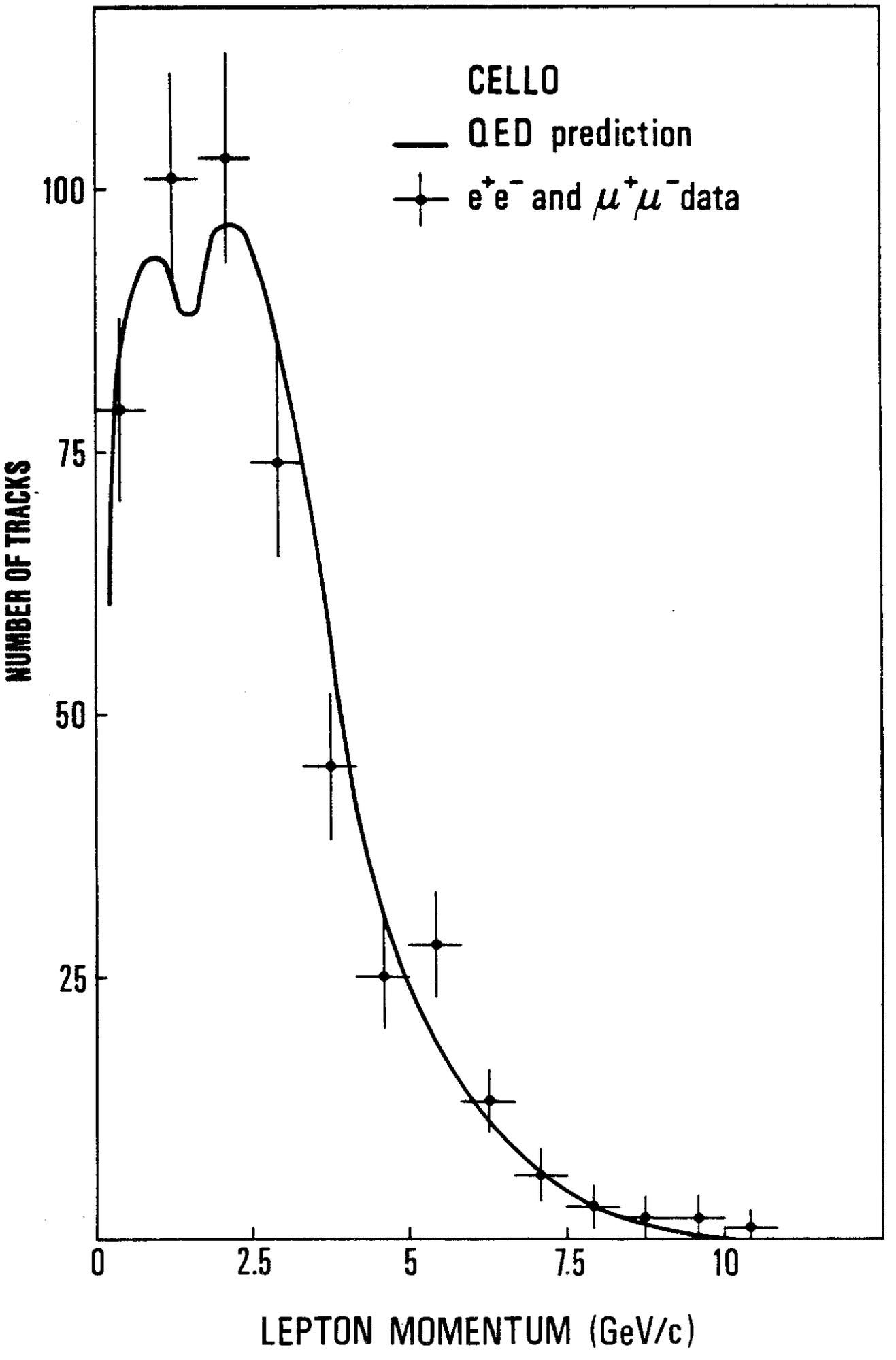
CELLO
QED prediction
e^+e^- and $\mu^+\mu^-$ data
NUMBER OF TRACKS
100
75
50
25
0
2.5
5
7.5
10
LEPTON MOMENTUM (GeV/c)

Fig. 2a

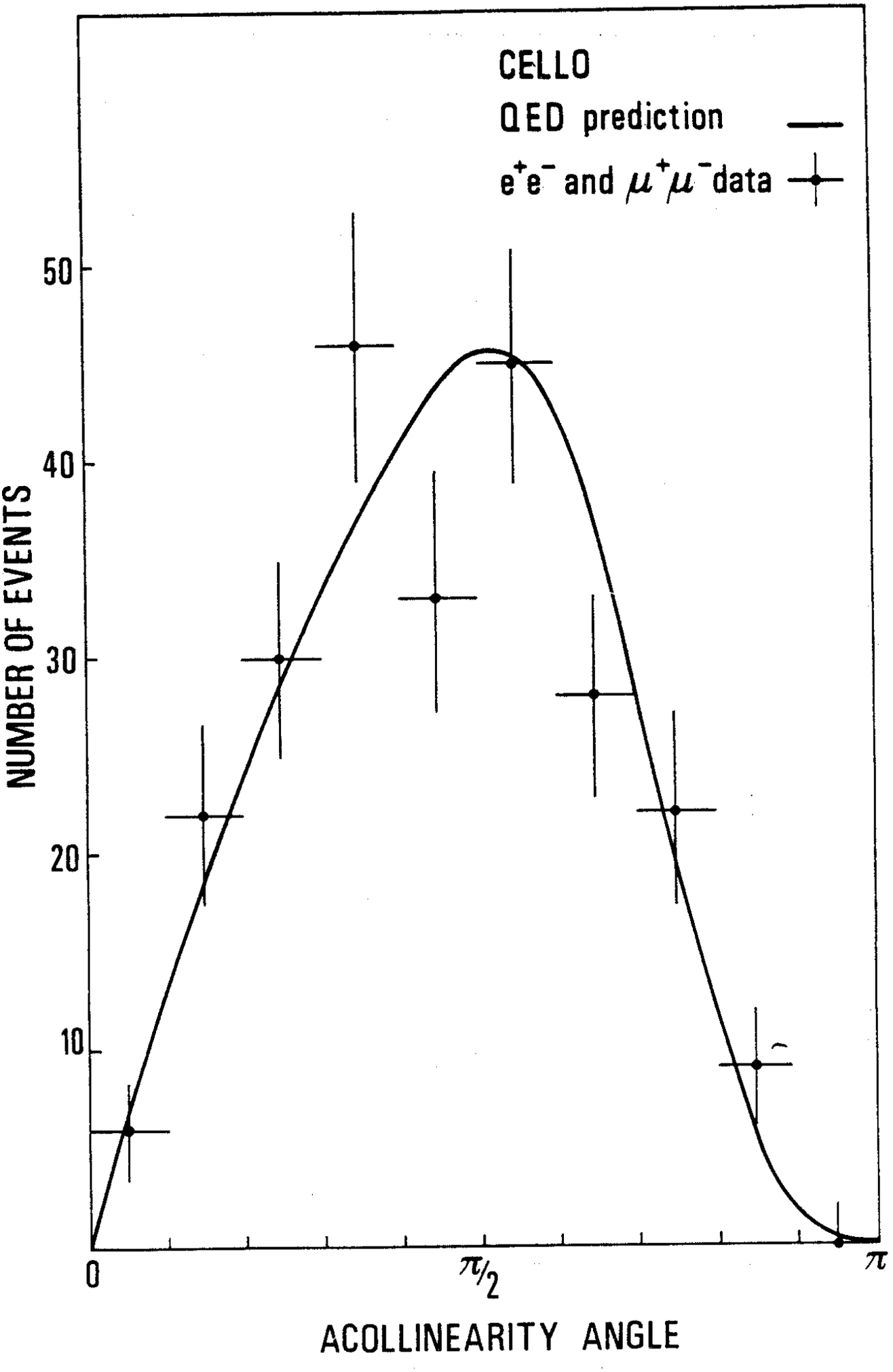
CELLO
QED prediction
e^+e^- and $\mu^+\mu^-$ data
NUMBER OF EVENTS
50
40
30
20
10
0
$\pi/2$
π
ACOLLINEARITY ANGLE

Fig. 2b

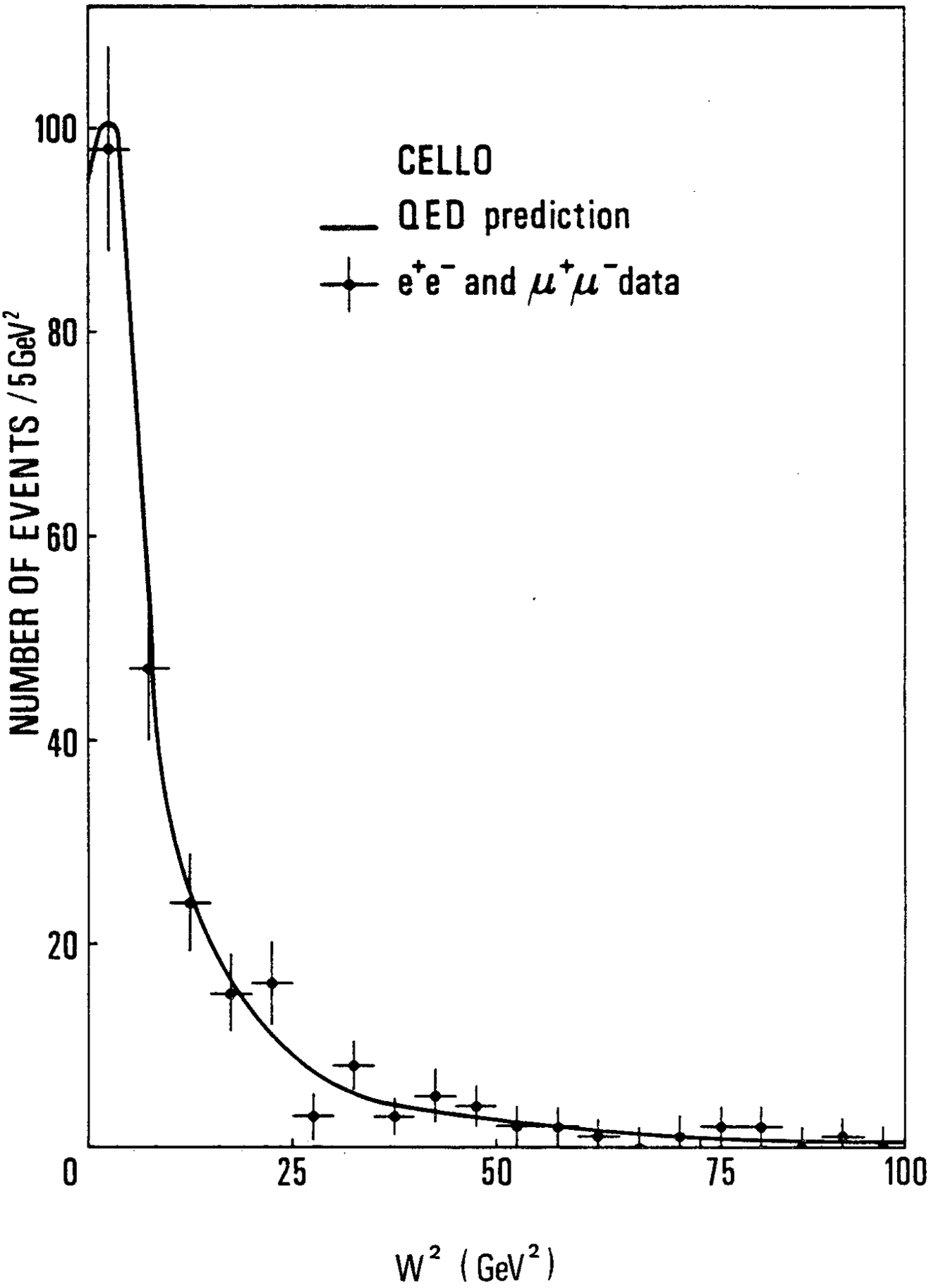
CELLO
QED prediction
e+e- and μ+μ- data
NUMBER OF EVENTS /5GeV²
100
80
60
40
20
0
25
50
75
100
W² (GeV²)

Fig. 3a

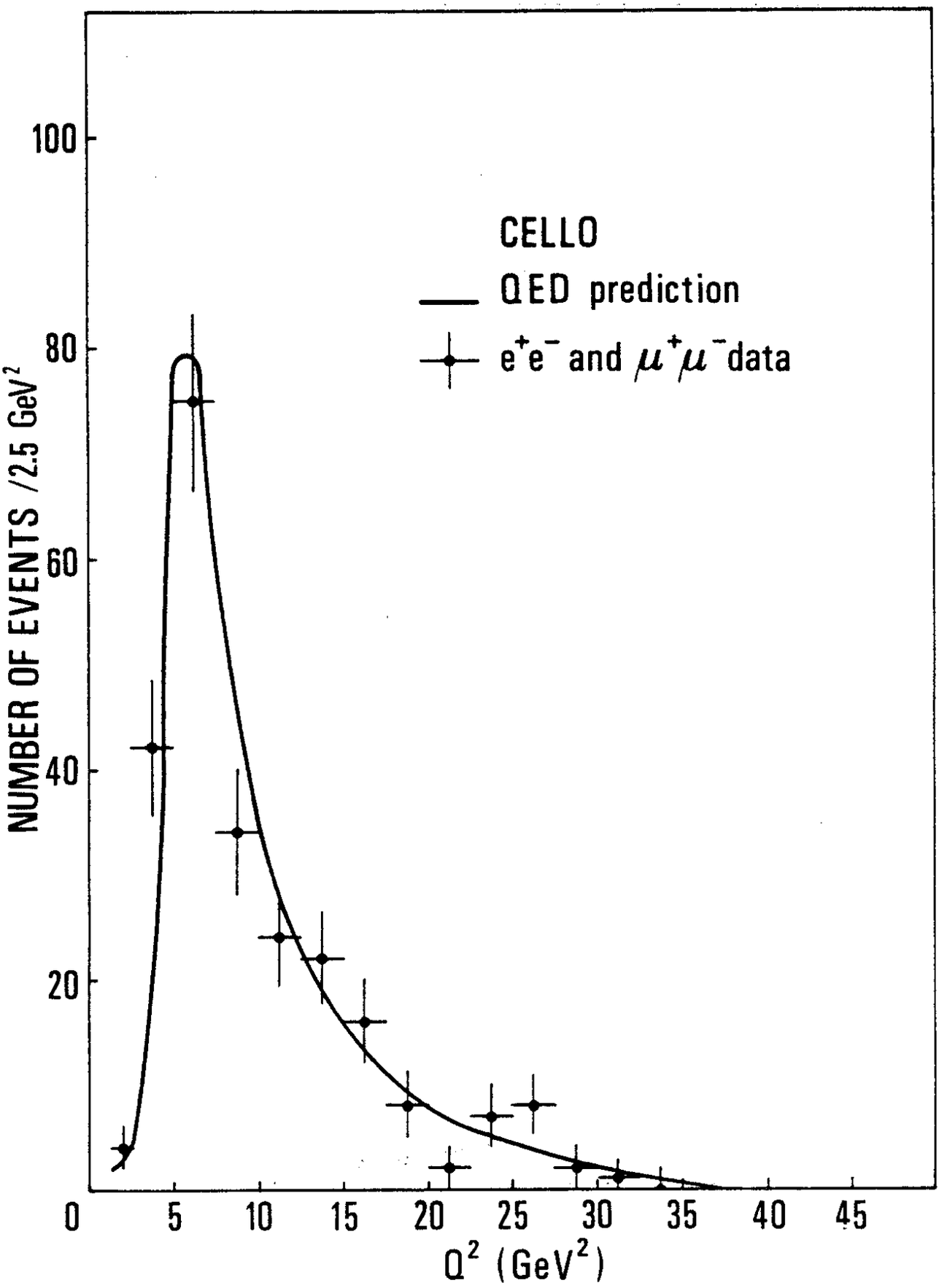
CELLO
QED prediction
e+e− and μ+μ− data
NUMBER OF EVENTS /2.5 GeV²
Q² (GeV²)
0
5
10
15
20
25
30
35
40
45
20
40
60
80
100

Fig. 3b

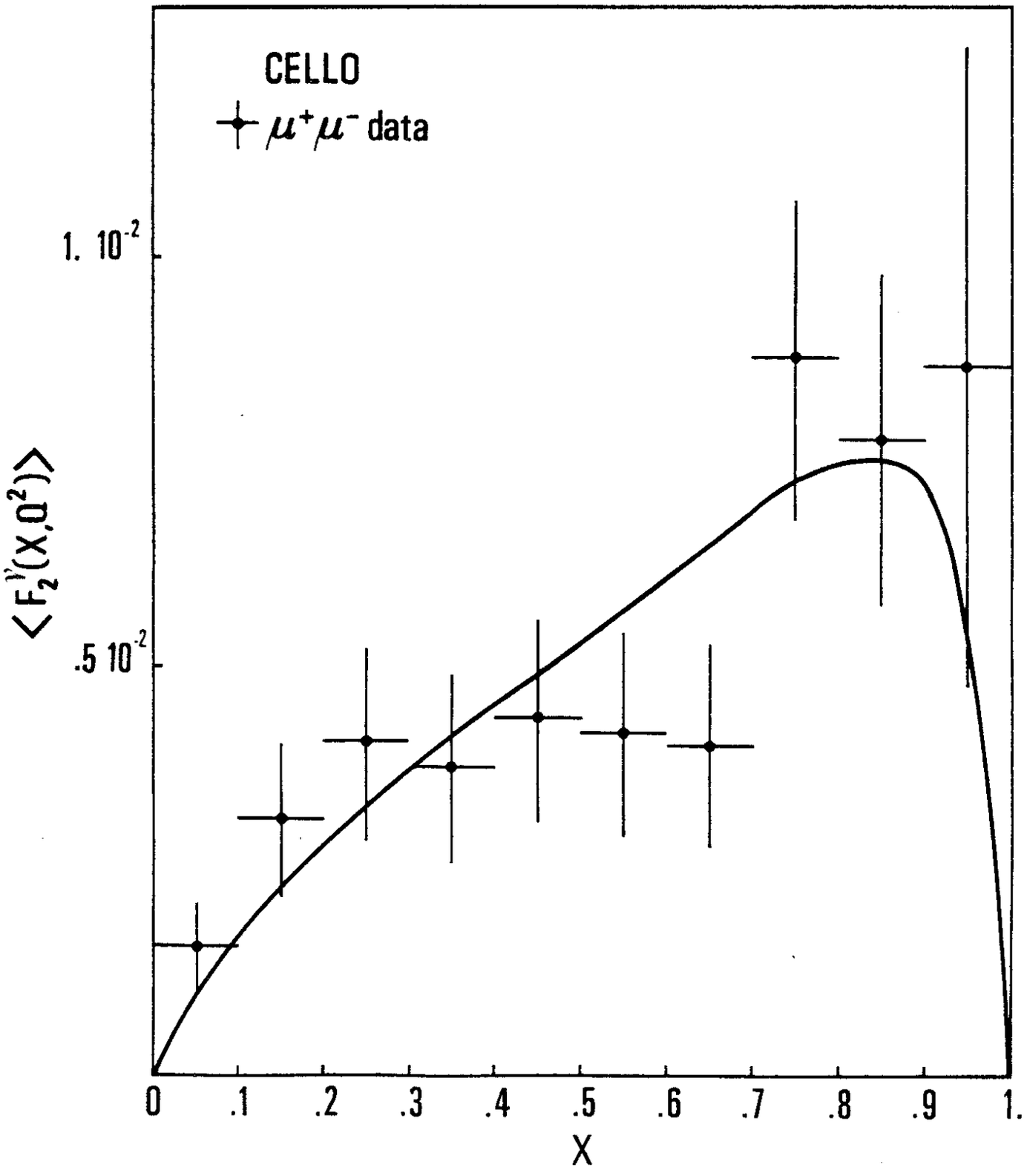
CELLO
$\mu^+\mu^-$ data
1. 10^{-2}
.5 10^{-2}
$\langle F_2^{\gamma}(X,Q^2)\rangle$
0
.1
.2
.3
.4
.5
.6
.7
.8
.9
1.
X

Fig. 4